Signal Processing 176 (2020) 107686

Contents lists available at ScienceDirect

Signal Processing

journal homepage: www.elsevier.com/locate/sigpro

Short communication

Median ensemble empirical mode decomposition

Xun Lang[a], Naveed ur Rehman[b], Yufeng Zhang[a,*], Lei Xie[c], Hongye Su[c]

[a] Department of Electronic Engineering, Information School, Yunnan University, Kunming 650091, China
[b] Department of Electrical and Computer Engineering, COMSATS University Islamabad, Islamabad 45550, Pakistan
[c] State Key Laboratory of Industrial Control Technology, Zhejiang University, Hangzhou 310027, China

ARTICLE INFO

Article history:
Received 3 December 2019
Revised 25 May 2020
Accepted 2 June 2020
Available online 4 June 2020

Keywords:
Empirical mode decomposition
Ensemble empirical mode decomposition
Mode splitting
Median

ABSTRACT

Ensemble empirical mode decomposition (EEMD) belongs to a class of noise-assisted EMD methods that are aimed at alleviating mode mixing caused by noise and signal intermittency. In this work, we propose a median ensembled version of EEMD (MEEMD) to help reduce the additional mode splitting problem of the original EEMD algorithm. That is achieved by replacing the mean operator with the median operator during the ensemble process. Our use of the median operator is motivated by a rigorous analysis of mode splitting rates for both EEMD and MEEMD. It is shown that EEMD comes with irremovable new mode splitting while the proposed method can greatly reduce this problem on a breakdown point of 50%. This work is verified by extensive numerical examples as well as industrial oscillation case in terms of reducing the mode splitting.

© 2020 Elsevier B.V. All rights reserved.

1. Introduction

Empirical mode decomposition (EMD) [1] is currently one of the most powerful tools for performing time-frequency (T-F) analysis [2,3]. Within EMD, the input data is adaptively decomposed into a set of intrinsic mode functions (IMFs), which yield meaningful instantaneous frequency estimates through the Hilbert transform [1]. Owing to its data-driven nature in addition to the ability of processing nonlinear and nonstationary data, EMD is widely applied in numerous engineering applications [4–6].

The frequent appearance of noise and signal intermittency in real-world data usually causes mode mixing and mode splitting (MS) in EMD, where mode mixing is defined as one IMF containing different scales, while MS refers to the spread of one scale over two or more IMFs [2]. To alleviate this problem, ensemble empirical mode decomposition (EEMD) has been proposed by performing the EMD over an ensemble of the signal plus white Gaussian noise (wGn) [7]. EEMD belongs to a class of noise-assisted EMD-based methods which further include complementary EEMD [8], complete EEMD [9,10], partly EEMD [11], and the noise-assisted multivariate EMD (MEMD) [3] and fast multivariate EMD (FMEMD) [12].

The addition of wGn alleviates the mode mixing problem by populating the whole time-frequency space to take advantage of the self-similar filter bank behavior of EMD for broad band processes [13,14], however it inevitably creates new MS due to two main reasons: (i) Signals having a scale located in the overlapping region of the EMD equivalent filter would have a finite probability of mode splitting [7]; (ii) The added wGn cannot guarantee full uniformity across all scales, which may lead unexpected signal intermittency and irregularity [15].

To reduce the additional MS, we propose a variation of the EEMD algorithm that uses the median operator instead of the mean operator to ensemble noisy IMF trials. Our choice of using median within EEMD is not trivial or arbitrary. It is motivated by a rigorous study of the MS phenomena within the noise-assisted EMD based methods. To that end, we present novel probabilistic tools to quantify how MS appears. Then, after theoretically analyzing the ways of reducing the probability of additional MS, we finally choose to use the median operator, since it is the most robust alternative to the arithmetic mean. Moreover, a study of the effect of noise on completeness of the method as well as the results of a quantifying measure for MS reduction in MEEMD vs other noise-assisted EMD-based methods are given in detail. The effectiveness of the proposed method is finally verified on T-F analysis of the industrial oscillation signal.

2. Quantifying mode splitting of EEMD

In this section, we illustrate the MS phenomenon of EEMD by defining a series of probabilistic tools to quantify it. That would enable a rigorous performance comparison between existing noise-assisted EMD methods and then inspire our proposed approach. Since the ensemble IMF of EEMD is averaged from N indepen-

* Corresponding author.
E-mail addresses: zhangyf@ynu.edu.cn (Y. Zhang), leix@iipc.zju.edu.cn (L. Xie).

https://doi.org/10.1016/j.sigpro.2020.107686
0165-1684/© 2020 Elsevier B.V. All rights reserved.

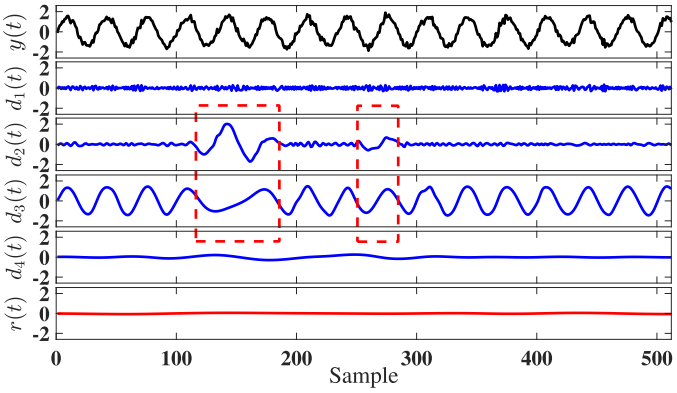

Fig. 1. An illustration of mode splitting. Note the splitting of a mode across $d_2(t)$ and $d_3(t)$ shown by the red rectangles. (For interpretation of the references to color in this figure legend, the reader is referred to the web version of this article.)

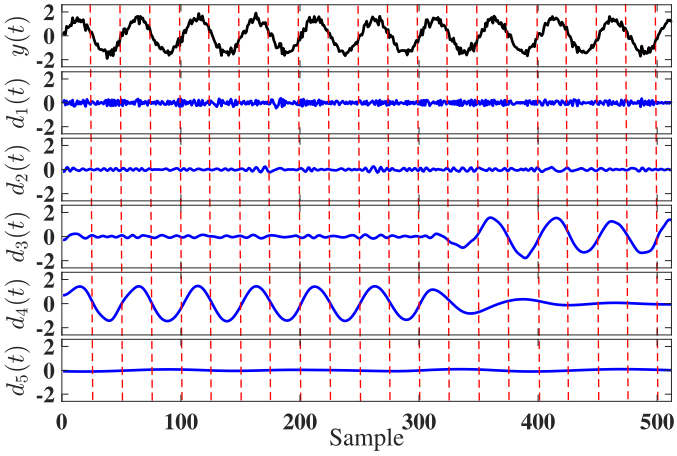

Fig. 2. Illustration of the dividing process in half-wave units. Notice that the incomplete half-wave at the end of the signal will be truncated.

dent EMD-based realizations, the MS phenomenon can be analyzed by setting ensemble size $N = 1$, without loss of generality. Taking $x(t) = \sin(2\pi ft)$ as an example, one realization of the signal plus noise in the EEMD process is

$$y(t) = \sin(2\pi ft) + \varepsilon w(t), \tag{1}$$

where $w(t) \sim \mathcal{N}(0, 1)$, ε denotes the amplitude of the added noise which usually takes a value of 0.2 times the standard deviation of $x(t)$ [7]. Here, the use of a pure tone $x(t)$ can greatly facilitate the subsequent analysis. From the EMD-based decomposition of $y(t)$, we can easily know which part of the decomposed IMF contains the sinusoidal signal.

By setting $f = 3$, $f_s = 100$ (sampling rate), $L = 512$ (data length) and $S = 5$ (stopping criterion for IMF extraction [16]), a typical decomposition of $y(t)$ via EMD is shown in Fig 1. Several important observations we made from the figure are in order:

(i) MS occurs in two separate intervals as highlighted by dashed boxes; (ii) Since EMD is totally extrema-driven and each half-wave of $x(t)$ contains only one extremum, the split oscillations mainly appear in half-wave units; (iii) The split oscillations and $x(t)$ have similar frequencies and morphological characteristics, indicating that MS can be quantified by setting the half-wave window of $x(t)$ as the unit; (iv) In comparison with the noise-only windows, the signal windows show greater magnitudes.

Based on the above observations, the phenomenon of MS can be analyzed statistically. Assume that $x(t)$ has $W_x(f)$ half-waves in total, divide each IMF into $W_x(f)$ windows based on the time information of the half-waves of $x(t)$ (a simple illustration of the dividing processing is shown in Fig. 2). Then if the sum of the absolutes of the samples in a window exceeds a certain threshold,[1] we conclude that part of $x(t)$ occurs in this window. For frequency interval [1.4, 4.9], we first define two important quantities:

$p_i(f)$: the probability of the presence of $x(t)$ in i-th IMF, where $i = 2, 3, 4$. For each f, it is calculated by estimating the percentage of 1000 independent realizations where there exists a window in i-th IMF above the threshold T_k.

$r_i(f)$: the duration (in %) of $x(t)$ in i-th IMF, given that $x(t)$ splits to that mode. In each independent realization, it is calculated as the ratio of $x(t)$ related half-wave windows in a mode ($W_i(f)$) to the total half-waves of $x(t)$, namely, $\frac{W_i(f)}{W_x(f)} \times 100\%$, where $W_i(f) \geq 1$. Essentially, $r_i(f)$ measures the conditional probability of the presence of $x(t)$ in any half-wave window of the i-th IMF, given the condition that $x(t)$ splits to that mode.

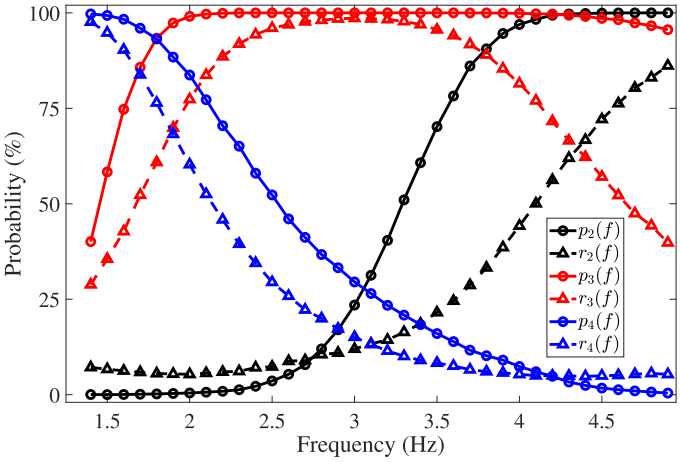

Fig. 3. Demonstration of the empirically estimated probabilistic curves for $p_i(f)$ and $r_i(f)$, where $i = 2, 3, 4$.

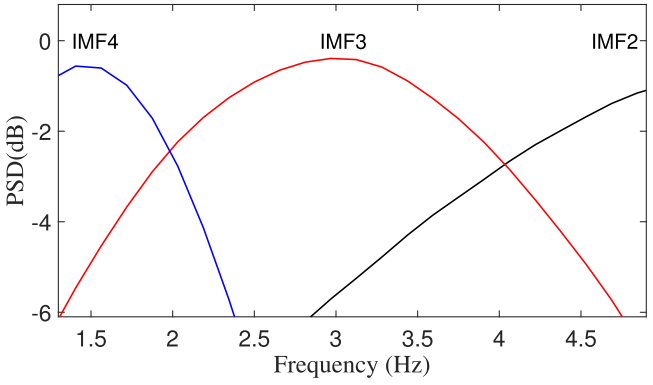

Fig. 4. The IMF spectra of the EMD equivalent filter in frequency interval [1.4, 4.9].

The fitted curves of above quantities associated with the frequency f are plotted in Fig. 3. In combination with the filter bank structure of EMD [13,14] shown in Fig. 4, it is concluded that: (i) When $x(t)$ resides in the intra-band region (with frequency close to the peak of IMF3 spectrum, $f = 3$ in Fig. 4), $p_3(f)$ and $r_3(f)$ keep

[1] We can use the noise component in the first IMF to calculate the thresholds for IMF2, IMF3 and IMF4. Assume that the averaged integral of the absolutes of samples in a half-wave window of IMF1 is $\bar{T}_1$, then this value for noise-only window in k-th IMF can be approximated as $\bar{T}_k = \frac{\bar{T}_1}{\sqrt{\beta}} \rho^{-\frac{k}{2}}, k = 2, 3, 4$, where the default values of β and ρ are 0.719 and 2.01, respectively [17,18]. Accordingly, we set the threshold as $T_k = 2 \cdot \bar{T}_k$ for k-th IMF to reduce the probability of determining a noise window as a signal window.

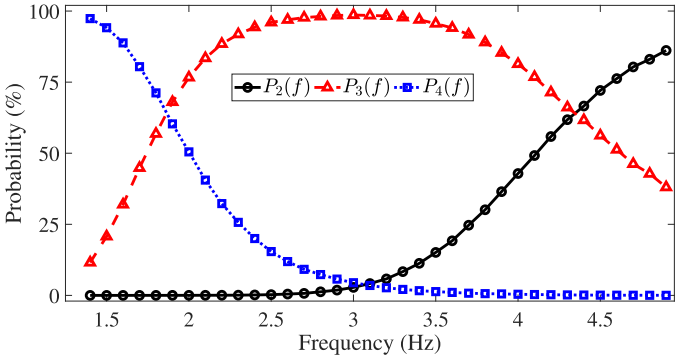

Fig. 5. Demonstration of the probabilistic curves $P_i(f)$ for a single EMD-based realization of the noise added signal within the EEMD process..

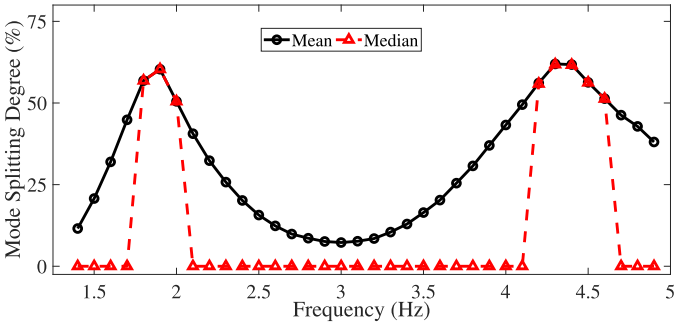

Fig. 6. Curves of the mode splitting degree $MSD(f)$ of the EEMD process for different ensemble operators.

steadily high. On the other hand, $p_2(f)$ and $r_2(f)$ (also $p_4(f)$ and $r_4(f)$) that corresponding to IMF2 (IMF4) exhibit low values, but do not decay to zero; (ii) when $x(t)$ moves to the overlapping region between adjacent IMF spectra (for example, with frequency close to $f = 4$) or even further away to adjacent intra-band (IMF2), $p_2(f)$ and $r_2(f)$ increase dramatically, even up to 100%. Similarly, $p_4(f)$ and $r_4(f)$ show the same growth when the frequency of $x(t)$ decreases towards 1 Hz. We highlight that $\sum_{i=2}^{4} p_i(f)$ and $\sum_{i=2}^{4} r_i(f)$ are usually greater than one. This is not conflict with their definitions, since $x(t)$ can ride across two adjacent IMFs even in a single half-wave window, e.g., the right box in Fig. 1. Also for this reason, EEMD divides $x(t)$ into two sinusoidal signals, which will be shown later in Fig. 7.

We next introduce a new definition as given by

$$P_i(f) = p_i(f) \cdot r_i(f), \tag{2}$$

for $i = 2, 3, 4$. Since $p_i(f)$ denotes the probability of the presence of $x(t)$ in i-th IMF and $r_i(f)$ measures the conditional probability of the duration (in %) of $x(t)$ in this mode, the idea behind (2) is clear, i.e., $P_i(f)$ represents the probability of the existence of $x(t)$ in any half-wave window of i-th IMF for each independent EMD-based realization. The curves of $P_i(f)$ are plotted in Fig. 5. Since all N realizations of EEMD are independent of each other, the subsequent mean operator in the ensemble process is unable to change these probabilities. As a result, $P_i(f) \times N$ of N realizations will above the threshold for each half-wave window in i-th IMF. If we define the percentage of realizations where $x(t)$ occurs as $PR_i(f)$, we finally have $PR_i(f) = \frac{P_i(f)\times N}{N} = P_i(f)$, which suggests that theoretically $PR_i(f)$ (in %) of the realizations will contain part of $x(t)$.

By using mean to complete the ensemble process, the amplitude of the ensembled IMF will be proportional to $PR_i(f)$. Therefore, $PR_i(f)$ can be further adopted to indicate the degree of $x(t)$ in the i-th IMF. Since EEMD is fully data-driven and mode splitting refers to the leakage of relatively few portions of $x(t)$ from a particular IMF to other IMFs, the mode with the highest degree of $x(t)$ (highest $PR_i(f)$) should be considered as the main scale, with other two IMFs being regarded as mode splitting ones. Accordingly, we define the mode splitting degree $MSD(f)$ as

$$MSD(f) = \sum_{i=2}^{4} PR_i(f) - \max\{PR_2(f), PR_3(f), PR_4(f)\} \tag{3}$$

where the higher the $MSD(f)$, the higher amplitude of the split IMFs, and the higher degree of mode splitting. For our test signal $x(t)$, the $MSD(f)$ of the original EEMD process is represented by the black solid-line in Fig. 6. It is observed that no matter how the frequency is tuned, there is always a non-zero degree of MS for the mean operator. In addition, the obtained curve is in agreement with the filter bank property of EMD (Fig. 4), more specifically: (i) When $x(t)$ is tuned into the intra-band of IMF3, most half-waves locate in this mode, yielding relatively low $MSD(f)$; (ii) When f moves to the overlapping bands, more and more half-waves split to adjacent modes, which results in rising $MSD(f)$ curve; (iii) When f shifts from the overlapping bands to adjacent intra-bands that corresponding to IMF2 and IMF4 (f close to 1.4 Hz and 4.9 Hz), most of the half-waves prefer to concentrate in IMF2 or IMF4, leading to gradually decreased $MSD(f)$ value.

However, if we use the median operator to analyze the ensemble process within EEMD, the modified process will have a breakdown point of 50%. For each half-wave window, as long as no more than half of the realizations contain $x(t)$, the median will not give an arbitrarily large or small result. Therefore, the $MSD(f)$ curve corresponding to the median-based EEMD can be obtained as shown in the red dashed-line of Fig. 6. As depicted, the median operator is able to reduce the MS probability for most of the cases. However, due to the fact that $x(t)$ may ride across two adjacent IMFs even in a single half-wave window, there exists certain case that two of the percentages in set $\{PR_i(f)\}_{i=2}^{4}$ are greater than 50%. In such scenario, our proposed MEEMD will lose its effectiveness in alleviating the mode splitting problem, as highlighted in Fig. 6.

3. Median EEMD and its property

We now propose the median EEMD (MEEMD) algorithm, where the median ensembled IMF is defined as [19]

$$\mathrm{IMF}^{\mathrm{median}}(t) = \frac{\mathrm{IMF}^{\lfloor (N+1)/2 \rfloor}(t) + \mathrm{IMF}^{\lceil (N+1)/2 \rceil}(t)}{2}, \tag{4}$$

in which $\mathrm{IMF}^n(t)$, $n = 1, 2, \ldots, N$ denotes the ordered IMF list at time instant t, which is obtained from N independent EMD based realizations. Consider a real-valued signal $x(t)$ and a predefined noise amplitude ε, the proposed MEEMD is outlined in Algorithm 1.

Algorithm 1 Algorithm of MEEMD.

1: Generate the ensemble $y_n(t) = x(t) + \varepsilon w_n(t)$ for $n = 1, \ldots, N$, where $w_n(t) \sim \mathcal{N}(0, 1)$;
2: Decompose every member of $y_n(t)$ into M_n IMFs using the standard EMD, to yield the IMF set $\{d_m^n(t)\}_{m=1}^{M_n}$;
3: Assemble same-index IMFs across the ensemble using the median operator to obtain the final IMFs within MEEMD; for instance, the m-th IMF is computed as $d_m(t) = \mathrm{median}\left\{d_m^1(t), d_m^2(t), \ldots, d_m^N(t)\right\}$.

The enhanced performance of the proposed method in alleviating the additional MS problem is exemplified by taking $x(t) = \cos(2\pi f t)$ as an illustration. According to Fig. 6, different frequencies of $x(t)$ will lead to different $MSD(f)$ values, i.e., different degrees of mode splitting. Without loss of generality, we set $f = 3.5$,

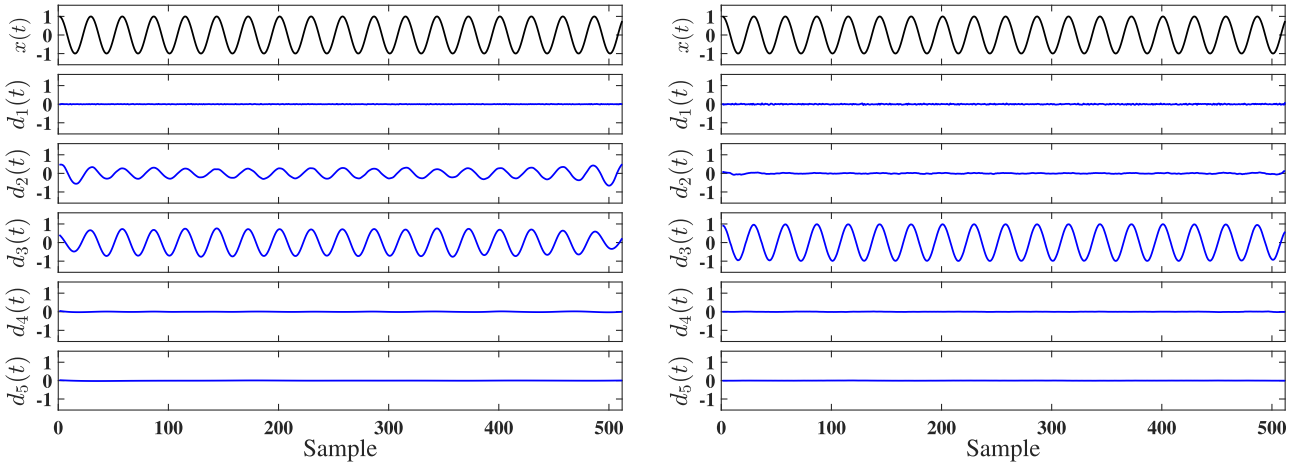

Fig. 7. Decomposition of signal $x(t)$ via: EEMD (left) and MEEMD (right). For simplicity, we have plotted the first five IMFs only.

$f_s = 100$, $L = 512$, $N = 100$ and $\varepsilon = 0.2\text{std}\{x(t)\}$. The decomposition results obtained from both EEMD and MEEMD methods are plotted in Fig. 7. In this case, EEMD shows non-negligible MS phenomenon, which compromises the practicality of the EEMD extensions in real-world applications. In contrast, the decomposition results of MEEMD provide more clear and accurate picture on the underlying data structure of $x(t)$.

3.1. The effect of noise on completeness of MEEMD

For normal distribution $\mathcal{N}(\mu, \varepsilon^2)$, its median is asymptotically normal with mean m and variance [20]: $\sigma^2 = 1/\left[4Ng(m)^2\right]$, where $g(\cdot)$ is the probability density function of the normal distribution, and N is the sample size. Accordingly, we can obtain the variance of the median samples by combining with the median of the normal distribution ($m = \mu = 0$), as $\sigma^2(0) = \frac{1}{4Ng(0)^2} = \frac{\pi}{2N}\varepsilon^2$. As a result, the effect of the added noise for MEEMD should follow the statistical rule:

$$\sigma_N = \sqrt{\frac{\pi}{2N}}\varepsilon, \tag{5}$$

where σ_N is the final standard deviation of error, which is defined as the difference between the input signal and the sum of the corresponding IMFs. Compared to the statistical rule of EEMD given by [7] ($\sigma_N = \frac{\varepsilon}{\sqrt{N}}$), the noise residual of the proposed MEEMD is consistently greater than that of the EEMD method for the same N, with a multiple of $\sqrt{\frac{\pi}{2}}$. This analysis highlights that: to ensure the similar completeness, the ensemble size of MEEMD should be roughly 1.25 times greater than that of EEMD. To demonstrate the above analysis, $x(t) = \cos(2\pi ft)$ with $f = 3$, $f_s = 100$ and $L = 512$ is adopted to check whether the final standard deviation of error is consistent with the theoretical value. First, we introduce a new quantity as given by

$$SDR(N) = \frac{\sigma_N}{\varepsilon}, \tag{6}$$

in which $\sigma_N = \text{std}\left\{x(t) - \sum_{i=1}^{M} d_i^N(t)\right\}$, where $\left\{d_i^N(t)\right\}_{i=1}^{M}$ denote the M sets of IMFs obtained from EEMD/MEEMD with ensemble size N, and $\varepsilon = 0.2\text{std}\{x(t)\}$ according to [7]. Theoretically, the $SDR(N)$ values for EEMD and MEEMD are $\frac{1}{\sqrt{N}}$ and $\sqrt{\frac{\pi}{2N}}$, respectively. To test the noise residual of EEMD versus MEEMD as N increases, we perform the experiments from $N = 5$ to 100, with an interval of 5. Their $SDR(N)$ curves are finally averaged from 1000 independent realizations, yielding the comparative results as shown in Fig. 8. As depicted, the experimental results are almost in line with their theoretical curves for both EEMD and MEEMD.

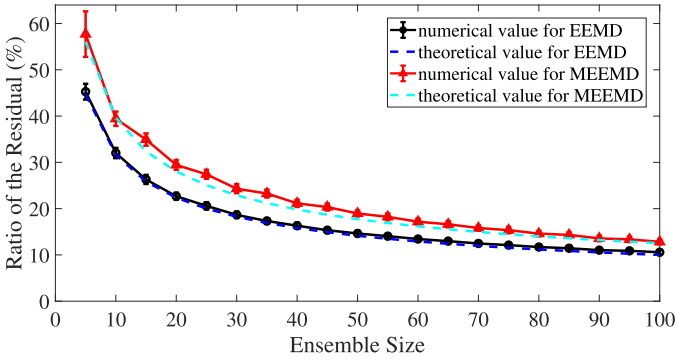

Fig. 8. $SDR(N)$ curves for different ensemble sizes within EEMD and MEEMD.

3.2. Mode splitting reduction of MEEMD vs EEMD

Here we demonstrate the superiority of MEEMD in reducing the MS problem by analyzing signal $x(t) = \cos(2\pi ft)$ statistically. To quantify the extent to which the split portion of the signal is proportional to the original signal, we define the mode splitting ratio as follows

$$R(f) = \frac{\int_T \left[|d_{k-1}(t)| + |d_{k+1}(t)|\right]\text{d}t}{\int_T |x(t)|\text{d}t}, \tag{7}$$

where $k = \arg\max_i \{\int |d_i(t)|\text{d}t\}$, $i = 2, \ldots, M-1$ (M is number of the IMFs). Owing to the ensemble process, the noise residual has small effect on the integral of the mode. Since $d_k(t)$ contains most of the portions of $x(t)$, $R(f)$ can be a natural indication of the degree of mode splitting. Accordingly, the larger the $R(f)$ value, the more severe the method is affected by mode splitting. Both methods are initialized with $\varepsilon = 0.2\text{std}\{x(t)\}$ and $L = 512$. However, to test the performance of MEEMD versus EEMD as N increases, we acted the experiments with different ensemble sizes, i.e., $N = 3$, 5, 10, 20, 50 and 100, respectively. Their $R(f)$ curves with $T \in [0, 5.12]$ are averaged from 1000 independent realizations, yielding a set of comparative results shown in Fig. 9. We observe that the obtained results of $R(f)$ are highly consistent with the $MSD(f)$ curves given in Fig. 6. In comparison with EEMD, the proposed MEEMD method shows considerable superiority in alleviating the MS problem for different values of N. With regard to their variances, both methods exhibit decreased variances as the ensemble size increases. On the contrary, they show increased variances when the $R(f)$ value increases.

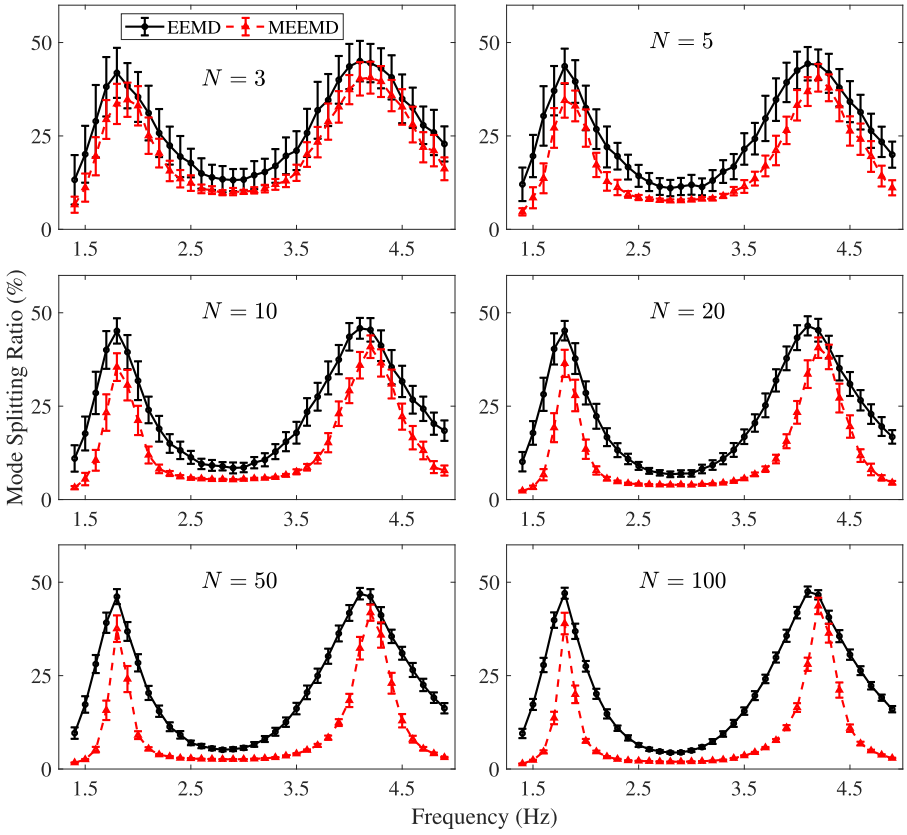

Fig. 9. $R(f)$ curves for different ensemble sizes within EEMD and MEEMD.

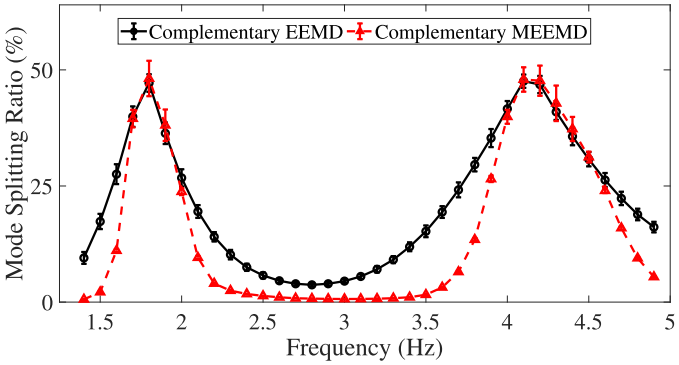

Fig. 10. $R(f)$ curves within the complementary EEMD and MEEMD.

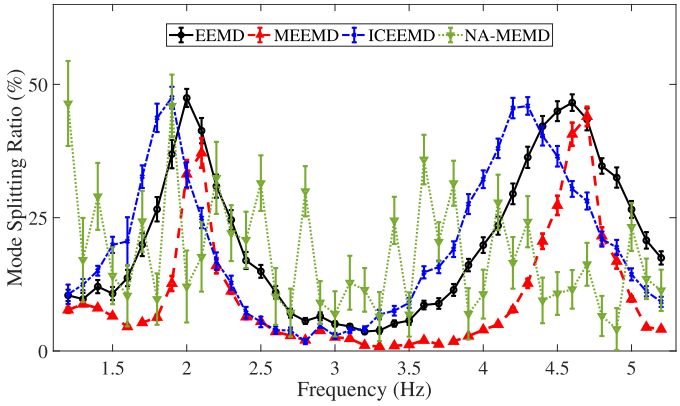

Fig. 11. Curves of $R(f)$ for different noise-assisted methods.

In this work, the complementary versions [8] of EEMD and MEEMD are also compared, where the complementary MEEMD is constructed by: $d_m(t) = \text{median}\left\{\frac{d_m^{1+}(t)+d_m^{1-}(t)}{2}, \ldots, \frac{d_m^{N+}(t)+d_m^{N-}(t)}{2}\right\}$, in which $d_m^{n+}(t)$ and $d_m^{n-}(t)$ represent a pair of IMFs obtained from the mixtures of signal with positive and negative noises. The computed $R(f)$ curves are given in Fig. 10, where the ensemble sizes of both methods are limited to $N = 100$.

In this case, the effect of noise for the complementary MEEMD is completely removed under frequency interval $2.5 < f < 3.5$, however, it exhibits a significant performance degradation at the overlapping bands of the equivalent filter. One possible reason is that the mean process $\frac{d_m^{n+}(t)+d_m^{n-}(t)}{2}$ has led to an increase of $MSD(f)$ for MEEMD.

3.3. Comparative study

To further demonstrate the capability of MEEMD, a more complicated example is analyzed, where the signal is given by

$$z(t) = \cos(2\pi f t) + \beta w(t) \cdot \exp\left[-(t-5)^2/0.5\right], \tag{8}$$

in which β denotes the amplitude of noise $w(t) \sim \mathcal{N}(0,1)$, and $\exp\left[-(t-5)^2/0.5\right]$ controls the transient window of the noise component. In this study, $z(t)$ is tuned with $\beta = 1.0$, $f_s = 100$, and $L = 1024$, which is a general form of the two-tones signal. We then compare MEEMD with other related noise-assisted methods including EEMD, the improved complete EEMD (ICEEMD) [10] and the noise-assisted MEMD (NA-MEMD) [21], by using (7) as the

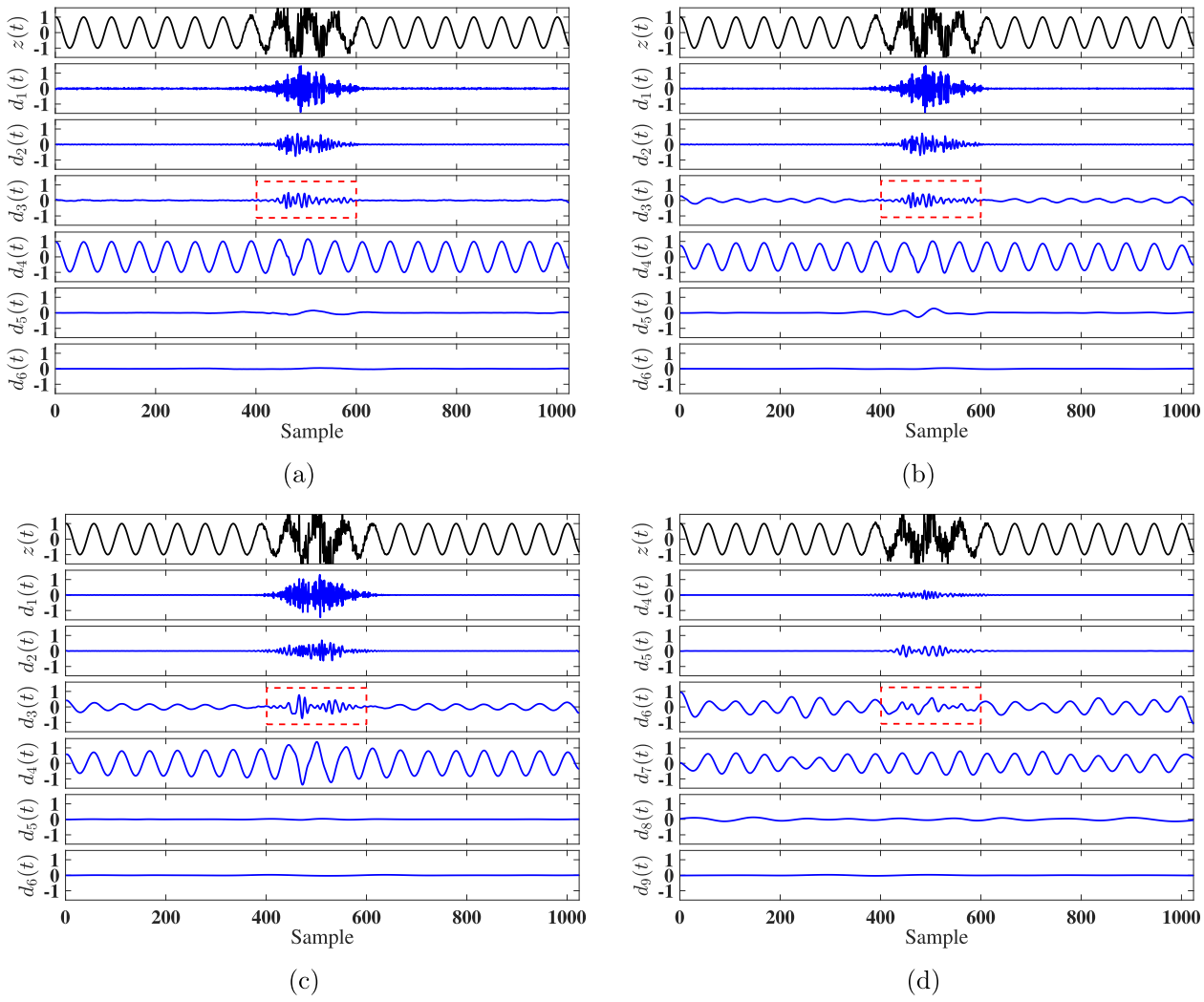

Fig. 12. Typical decomposition of signal $z(t)$ with $f = 1.8$ using: (a) MEEMD, (b) EEMD, (c) ICEEMD and (d) NA-MEMD. For simplicity, we have only plotted six selected IMFs in these figures (the first six IMFs for MEEMD, EEMD, ICEEMD and IMF4 to IMF9 for NA-MEMD). As highlighted in dashed boxes, the $R(f)$ measure will be significantly affected by the noise component from signal $w(t)$ in interval $T \in [4, 6]$.

quantitative measure in the task of extracting $\cos(2\pi ft)$ from $z(t)$.[2] Their $R(f)$ curves over frequency interval [1.2, 5.2] are averaged from 1000 independent realizations, where Fig. 11 shows the obtained results. It is observed that the proposed MEEMD shows the lowest mode splitting ratio for most of the frequency values. Moreover, its mean $R(f)$ value (MEEMD: 9.86) is roughly half of the other methods (EEMD: 20.42; ICEEMD: 19.53; NA-MEMD: 18.05), further demonstrating the usefulness of the proposed method. Finally, the variance performance of ICEEMD is similar to that of EEMD. However, the NA-MEMD shows the highest variances for most of the frequencies.

Next, we draw typical decomposition results of signal $z(t)$ with $f = 1.8$ by using the above four methods as shown in Fig. 12. As depicted, except for the proposed MEEMD method, all other methods show significant MS problem by dividing the cosine signal into two adjacent IMFs. Such observation is expected because both ICEEMD and NA-MEMD are developed to achieve a negligible reconstruction error and the same number of modes for different realizations, however, not to reduce the presence of additional MS. This example highlights that the reduction of additional MS is not just a challenge for EEMD, but a challenge for most of the noise-assisted EMD methods. This example also demonstrates that there is no difference between MEEMD and other noise-assisted EMD extensions in restraining the mode mixing problem. However, if the MS can cause additional mode mixing ($d_3(t)$ in Fig. 12(b) and (c)), the proposed MEEMD may outperform EEMD and its extensions in reducing both mode splitting and mode mixing. We highlight that if the noise component in (8) is replaced by another tone (for example $w(t) = \cos(2\pi 8t)$), the obtained results also support this analysis.

4. Industrial case study

We finally present a case study on T-F analysis of the industrial oscillation, where the nonlinear series is sampled from the output of an analyzer control loop every 36 seconds [22,23]. Both EEMD and MEEMD are included to process the oscillation with config-

[2] These methods are initialized with $N = 100$, $\varepsilon = 0.2\text{std}\{x(t)\}$, SNRFlag=1 (ICEEMD shows worse result with SNRFlag=2), $p = 48$ (direction vectors) and $q = 3$ (noise channels). For the adopted $R(f)$ measure, the investigated tone is $x(t) = \cos(2\pi ft)$. As highlighted in dashed boxes of Fig. 12, if we set $T \in [0, 10.24]$, then $R(f)$ will be significantly affected by the noise component from $w(t)$. Therefore, to minimize the impact of noise on the calculation of the mode splitting ratio, T is designated to $[0, 4] \cup [6, 10.24]$ in this example.

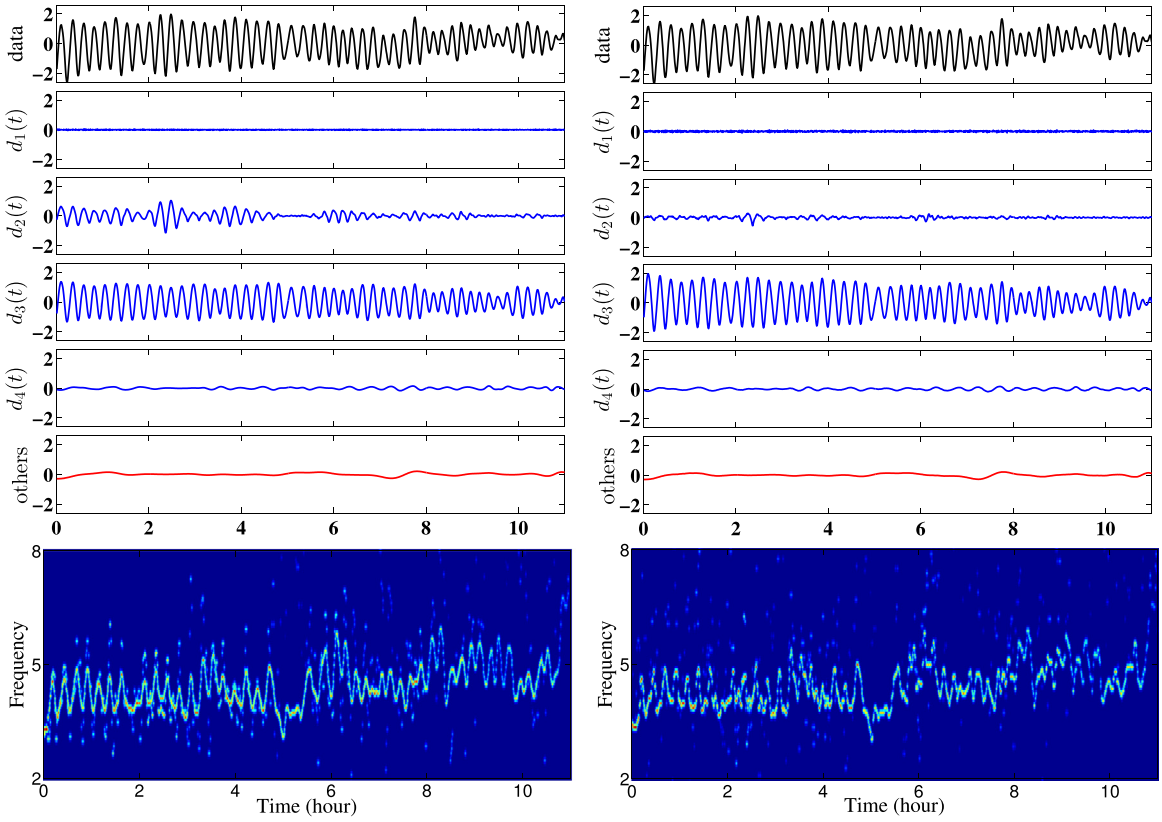

Fig. 13. Time-frequency analysis of the industrial oscillation via: EEMD (left) and MEEMD (right). For the decomposition plots, the top row is the original data, $d_1(t)$ to $d_4(t)$ denote the first four IMFs, 'others' is the sum of non-significant IMFs and the final trend. The bottom plots are illustration of the Hilbert spectra where the frequency is measured using 'cycles per hour'.

Table 1
Pearson correlation measures of adjacent IMFs.

Methods	r_{12}	r_{23}	r_{34}	r_{45}	r_{56}	r_{67}
EEMD	0.052 ± 0.012	0.830 ± 0.020	0.082 ± 0.016	0.270 ± 0.022	0.342 ± 0.030	0.388 ± 0.035
MEEMD	0.065 ± 0.020	0.602 ± 0.093	0.040 ± 0.007	0.256 ± 0.022	0.302 ± 0.030	0.288 ± 0.032

uration: $N = 100$, $L = 1100$ and $\varepsilon = 0.2\text{std}\{data\}$. The obtained results are shown in Fig. 13. We observe that EEMD performs worse than MEEMD and separates the oscillation into two IMFs ($d_2(t)$ and $d_3(t)$), which increases the difficulty of oscillation detection [24]. Moreover, the improved performance of MEEMD is specifically highlighted in the corresponding T-F plot where MEEMD shows better power concentration, resolution and lesser noise artifacts.

We next study the performance of both methods using the Pearson correlation coefficient for computing the similarity between any pair of the adjacent IMFs. In practical sense, the larger the Pearson correlation, the more severe the method is affected by MS. For the oscillation data, 1000 independent realizations of EEMD and MEEMD are carried out. Then, for each pair of the adjacent IMFs, the correlation measures are computed and averaged to yield the mean and standard deviation, as listed in Table 1. It can be noticed that both methods show particularly high correlation/similarity between IMF2 and IMF3. However, the proposed method exhibits much smaller value. This real-world case illustrates the inherent robustness of MEEMD to the mode-splitting problem. Though not included in this paper due to the lack of space, we also found that both ICEEMD and NA-MEMD observe non-negligible MS in processing this industrial data, which is similar to EEMD.

5. Conclusion and discussion

We have proposed to employ median operator within EEMD for signal decomposition. The performance improvement of the proposed approach has been demonstrated through extensive experiments and by utilizing a novel probabilistic framework to quantify mode splitting. This work is the first attempt to replace the mean operator of EEMD during the ensemble process. However, to achieve the special decomposition of the real-world signal, one can employ more advanced average operators such as mode, geometric or weighted mean. The extension to the complete algorithm with adaptive noise is also promising since it guarantees better completeness and lower computational cost.

Declaration of Competing Interest

The authors declare that they have no known competing financial interests or personal relationships that could have appeared to influence the work reported in this paper.

CRediT authorship contribution statement

Xun Lang: Conceptualization, Methodology, Software, Writing - original draft, Writing - review & editing. **Naveed ur Rehman:**

Methodology, Writing - review & editing. **Yufeng Zhang:** Validation, Software, Funding acquisition. **Lei Xie:** Validation, Writing - original draft, Writing - review & editing. **Hongye Su:** Validation, Writing - review & editing, Funding acquisition.

Acknowledgment

This work was supported in part by National Key R&D Program of China under Grant 2018YFB1701102 and National Natural Science Foundation of P.R. China under Grant 81771928.

Supplementary material

Supplementary material associated with this article can be found, in the online version, at doi:10.1016/j.sigpro.2020.107686.

References

[1] N.E. Huang, Z. Shen, S.R. Long, M.C. Wu, H.H. Shih, Q. Zheng, N.-C. Yen, C.C. Tung, H.H. Liu, The empirical mode decomposition and the hilbert spectrum for nonlinear and non-stationary time series analysis, in: Proceedings of the Royal Society of London A: Mathematical, Physical and Engineering Sciences, 454, The Royal Society, 1998, pp. 903–995.
[2] D.P. Mandic, N. ur Rehman, Z. Wu, N.E. Huang, Empirical mode decomposition-based time-frequency analysis of multivariate signals: the power of adaptive data analysis, IEEE Signal Process. Mag. 30 (6) (2013) 74–86.
[3] N. ur Rehman, D.P. Mandic, Multivariate empirical mode decomposition, in: Proceedings of the Royal Society of London A: Mathematical, Physical and Engineering Sciences, The Royal Society, 2009. rspa20090502
[4] K.T. Sweeney, S.F. McLoone, T.E. Ward, The use of ensemble empirical mode decomposition with canonical correlation analysis as a novel artifact removal technique, IEEE Trans. Biomed. Eng. 60 (1) (2012) 97–105.
[5] S.M.U. Abdullah, N. ur Rehman, M.M. Khan, D.P. Mandic, A multivariate empirical mode decompositionbased approach to pansharpening, IEEE Trans. Geosci. Remote Sens. 53 (7) (2015) 3974–3984.
[6] A. Zahra, N. Kanwal, N. ur Rehman, S. Ehsan, K.D. McDonald-Maier, Seizure detection from eeg signals using multivariate empirical mode decomposition, Comput. Biol. Med. 88 (2017) 132–141.
[7] Z. Wu, N.E. Huang, Ensemble empirical mode decomposition: a noise-assisted data analysis method, Adv. Adapt. Data Anal. 1 (1) (2009) 1–41.
[8] J.-R. Yeh, J.-S. Shieh, N.E. Huang, Complementary ensemble empirical mode decomposition: a novel noise enhanced data analysis method, Adv. Adapt. Data Anal. 2 (2) (2010) 135–156.
[9] M.E. Torres, M.A. Colominas, G. Schlotthauer, P. Flandrin, A complete ensemble empirical mode decomposition with adaptive noise, in: 2011 IEEE International Conference on Acoustics, Speech and Signal Processing (ICASSP), IEEE, 2011, pp. 4144–4147.
[10] M.A. Colominas, G. Schlotthauer, M.E. Torres, Improved complete ensemble emd: a suitable tool for biomedical signal processing, Biomed. Signal Process. Control 14 (2014) 19–29.
[11] J. Zheng, J. Cheng, Y. Yang, Partly ensemble empirical mode decomposition: an improved noise-assisted method for eliminating mode mixing, Signal Process. 96 (2014) 362–374.
[12] X. Lang, Q. Zheng, Z. Zhang, S. Lu, L. Xie, A. Horch, H. Su, Fast multivariate empirical mode decomposition, IEEE Access 6 (2018) 65521–65538.
[13] P. Flandrin, G. Rilling, P. Goncalves, Empirical mode decomposition as a filter bank, IEEE Signal Process. Lett. 11 (2) (2004) 112–114.
[14] Z. Wu, N.E. Huang, A study of the characteristics of white noise using the empirical mode decomposition method, Proc. R. Soc. Lond. Ser.A 460 (2046) (2004) 1597–1611.
[15] L. Xie, X. Lang, A. Horch, Y. Yang, Online oscillation detection in the presence of signal intermittency, Control Eng. Pract. 55 (2016) 91–100.
[16] N.E. Huang, M.-L.C. Wu, S.R. Long, S.S. Shen, W. Qu, P. Gloersen, K.L. Fan, A confidence limit for the empirical mode decomposition and hilbert spectral analysis, in: Proceedings of the Royal Society of London A: Mathematical, Physical and Engineering Sciences, 459, The Royal Society, 2003, pp. 2317–2345.
[17] Y. Kopsinis, S. McLaughlin, Development of emd-based denoising methods inspired by wavelet thresholding, IEEE Trans. Signal Process. 57 (4) (2009) 1351–1362.
[18] P. Flandrin, P. Gonçalves, G. Rilling, Emd equivalent filter banks, from interpretation to applications, in: Hilbert–Huang Transform and Its Applications, World Scientific, 2014, pp. 99–116.
[19] D.J. Sheskin, Handbook of parametric and nonparametric statistical procedures, crc Press, 2003.
[20] P.R. Rider, Variance of the median of small samples from several special populations, J. Am. Stat. Assoc. 55 (289) (1960) 148–150.
[21] N. ur Rehman, D.P. Mandic, Filter bank property of multivariate empirical mode decomposition, IEEE Trans. Signal Process. 59 (5) (2011) 2421–2426.
[22] M. Jelali, B. Huang, Detection and Diagnosis of Stiction in Control Loops: State of the Art and Advanced Methods, Springer Science & Business Media, 2009.
[23] Q. Chen, X. Lang, L. Xie, H. Su, Detecting nonlinear oscillations in process control loop based on an improved vmd, IEEE Access 7 (2019) 91446–91462.
[24] X. Lang, Z. Zhang, L. Xie, A. Horch, H. Su, Time-frequency analysis of plant-wide oscillations using multivariate intrinsic time-scale decomposition, Ind. Eng. Chem. Res. 57 (3) (2018) 954–966.